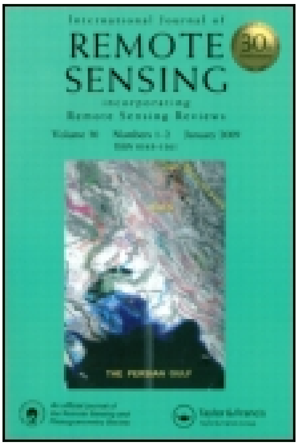

International Journal of Remote Sensing
Publication details, including instructions for authors and subscription information:
http://www.tandfonline.com/loi/tres20

Evaluation of radiative transfer models in atmospheric profiling with broadband infrared radiance measurements

Xin Jin [a], Jun Li [a], Timothy J. Schmit [b] & Mitchell D. Goldberg [b]

[a] Cooperative Institute for Meteorological Satellite Studies (CIMSS), University of Wisconsin-Madison, Madison, WI, USA

[b] Center for Satellite Applications and Research, NESDIS, NOAA, Camp Springs, MD, USA

Version of record first published: 26 Feb 2011

To cite this article: Xin Jin, Jun Li, Timothy J. Schmit & Mitchell D. Goldberg (2011): Evaluation of radiative transfer models in atmospheric profiling with broadband infrared radiance measurements, International Journal of Remote Sensing, 32:3, 863-874

To link to this article: http://dx.doi.org/10.1080/01431161.2010.517801

International Journal of Remote Sensing
Vol. 32, No. 3, 10 February 2011, 863–874

Evaluation of radiative transfer models in atmospheric profiling with broadband infrared radiance measurements

XIN JIN*†, JUN LI†, TIMOTHY J. SCHMIT‡ and MITCHELL D. GOLDBERG‡

†Cooperative Institute for Meteorological Satellite Studies (CIMSS), University of Wisconsin–Madison, Madison WI, USA

‡Center for Satellite Applications and Research, NESDIS, NOAA, Camp Springs, MD, USA

The infrared (IR) profile sounding based on satellite observations is an irreplaceable technique to monitor global atmospheric moisture information with high spatial resolutions. The long-term record of satellite IR measurement provides invaluable information for global climate study. Radiative transfer models (RTMs) are key issues in the sounding technique. The community radiative transfer model (cRTM), radiative transfer for Television and Infrared Observation Satellite (TIROS) Operational Vertical Sounde (TOVS) (RTTOV) and pressure layer fast algorithm for atmospheric transmittances (PFAAST) are tested in the legacy atmospheric profile (LAP) retrieval algorithm for Geostationary Operational Environmental Satellite (GOES-R) advanced baseline image (ABI). The Meteosat Second Generation/Spinning Enhanced Visible and Infrared Image (MSG/SEVIRI) measurements are used as proxy in the RTM evaluation. It is found that cRTM has the best performance in brightness temperature simulation and the tangent linear scheme integrated in both cRTM and RTTOV is better than the currently used approximate analytic scheme in deriving Jacobian matrix.

1. Introduction

Water vapour (WV) accounts for the largest percentage of the greenhouse effect, between 36% and 66% for WV alone, and between 66% and 85% when factoring in clouds. As the most important of all greenhouse gases, WV is a key issue in climate studies (Kiehl and Trenberth 1997). Since the early 1990s, a large number of studies based on convectional data sets, such as operational radisonde, broadband satellite remote sensing, numerical weather simulation, and so on, have been conducted to figure out the critical importance of tropospheric WV to the climate system (e.g. Lindzen 1990, Shine and Sinha 1991, Wu *et al.* 1993, Del Genio *et al.* 1994, Peixoto and Oort 1996, Held and Soden 2000).

Most of the impact on the climate system by atmospheric WV comes from its mid-upper tropospheric (UT) component. Some studies (Shine and Sinha 1991, Schneider

*Corresponding author. Email: xjin@ssec.wisc.edu

International Journal of Remote Sensing
ISSN 0143-1161 print/ISSN 1366-5901 online

http://www.tandf.co.uk/journals
DOI: 10.1080/01431161.2010.517801

et al. 1999, Held and Soden 2000) have proven that the variations in WV in the cold UT can have a radiative effect comparable to or greater than equivalent changes in the lower troposphere despite containing a small fraction of the total column WV. The long-term trend of UT WV is therefore a critical index in climate change. Based on satellite radiance observation since the 1970s, it has been found that the trend of UT WV has had a strong connection with El Niño Southern Oscillation events in the past two decades (Bates *et al.* 1996, Qian *et al.* 1998, Bates and Jackson 2001). Considering the importance of UT WV in climate studies, an immediate concern is to derive a high-quality UT WV data set. Harries (1997) illustrated the impact of UT WV with data from two satellite experiments and discovered that uncertainties of only a few per cent in terms of our knowledge of the humidity distribution in the atmosphere could produce changes to the outgoing spectrum of a similar magnitude to that caused by doubling carbon dioxide in the atmosphere. Integrating unreliable satellite-retrieved WV into a general circulation model cannot properly simulate the climate evolution (Soden and Schroeder 2000).

Accurate measurement of UT WV on a global scale with high spatial resolution is difficult. Early studies focused on sparsely distributed radiosonde data sets (Gaffen *et al.* 1991, Gutzler 1992, Zhai and Eskridge 1997) whose accuracy is questionable. Recently, polar-orbited hyperspectral infrared (IR) sensors, such as Atmospheric Infrared Sounder (AIRS) and Infrared Atmospheric Sounding Interferometer (IASI), have been popular in retrieving high-quality WV, especially UT WV, information on a global scale with high spatial resolution (Aires *et al.* 2002, Divakarla *et al.* 2006). Dessler *et al.* (2008) illustrated that the calculated clear-sky top-of-atmosphere outgoing long-wave radiation from two radiative transfer models (RTMs) driven by moisture profiles retrieved from AIRS have excellent agreement with measurements from another satellite instruments, that is, the Clouds and the Earth's Radiant Energy System (CERES). However, the relatively short history of the hyperspectral data set limits its application in climate studies. Moreover, the polar-orbited instruments can only scan low latitudes twice a day, which is another limitation of its climatological application.

Geostationary satellites can provide very high spatial/temporal coverage and resolution. Some famous geostationary platforms, such as Meteosat, Geostationary Operational Environmental Satellite (GOES) and Geostationary Meteorological Satellite (GMS), have provided UT WV observations for decades (Rossow and Schiffer 1991, Randel *et al.* 1996, Picon *et al.* 2003). Most geostationary platforms are equipped with infrared (IR) instruments to measure WV based on the absorption effect of WV between 6.3 μm and 7.3 μm. Broadband IR sounders and imagers are two major types of instruments. Compared with hyperspectral IR sensors, broadband instruments obviously have lower accuracy and lower vertical resolution (Schmit *et al.* 2009).

The hyperspectral instruments will not be on board the next generation of GOES satellite (GOES-R). Instead, the advanced baseline imager (ABI) will be the only instrument to continue the duty of monitoring atmospheric WV (Schmit *et al.* 2005). Improving the retrieval accuracy of atmospheric WV through broadband instruments is critical to the task of monitoring the climate trend before the implementation of hyperspectral instruments on board geostationary satellites. A previous study has shown that it is possible to adopt the current GOES Sounder WV physical retrieval algorithm to ABI with comparable precision (Jin *et al.* 2008).

Although broadband IR instruments have only limited capability in WV retrieval, the effort to improve the retrieval never stops. In this paper, we present the results of our efforts to improve the WV physical retrieval algorithm. Since the success of physical retrieval depends deeply on two critical factors – the performance of RTM and the accuracy of the weighting function matrix (Jacobian) – this paper is organized based on our study of these two aspects.

In the application of atmospheric profile sounding using IR observations from geostationary platform, there are, in general, two major types of fast RTM schemes dealing with atmospheric absorber optical depths: the regression-based prediction of optical depths on a fixed pressure grid (FPG) or fixed absorber overburden grid (FAO) (Sherlock *et al*. 2003). The Pressure-Layer Fast Algorithm for Atmospheric Transmittance (PFAAST) model, which is used in the current GOES sounding operation (Hannon *et al*. 1996), and the Radiative Transfer for Television and Infrared Observation Satellite (TIROS) Operational Vertical Sounder (TOVS) (RTTOV) (Saunders *et al*. 2002) are both well-known FPG RTMs. The recently developed community Radiative Transfer Model (cRTM), which integrates the optical path transmittance (OPTRAN) model, is based on the FAO scheme (Han *et al*. 2006).

The calculation of the Jacobian matrix is another time-consuming task. Li (1994) developed an approximate analytic (AA) form to calculate the Jacobian matrix. Based on the monochrome assumption, it is a fast and efficient approach with reasonable accuracy when applied to the hyperspectral IR sounder radiance process. However, the accuracy is limited when applied to the broad IR sounder data retrieval (Huang *et al*. 2002). This approach can be used in retrieval processing when the linear model is not accompanied by the RTM, such as PFAAST. New RTMs like RTTOV and cRTM integrate a tangent linear (TL) method to calculate the Jacobian matrix. TL is a time-consuming scheme but is independent of the monochrome approximation. Considering the leap in computing ability, these RTMs, accompanied by the TL method for Jacobian matrix, are suitable candidates for the new version of legacy atmospheric profile (LAP) retrieval. In this paper, we have compared the LAP retrievals with cRTM, RTTOV version 9.2 and PFAAST respectively. The data from Spinning Enhanced Visible and Infrared Imager (SEVIRI) on board the Meteosat Second Generation (MSG) are used in the experiments.

2. Results and discussion

2.1 *Simulations*

Figure 1 shows the weighting functions (Jacobian) for two WV absorbing bands (6.3 μm and 7.3 μm) calculated with different schemes. RTTOV and cRTM have their model-accompanied Jacobians derived from the TL method, while PFAAST uses AA Jacobians (Li 1994, Li *et al*. 2000). The US 1976 standard atmospheric profile is used in the calculations with a fixed local zenith angle (LZA) of 0, a fixed surface skin temperature of 300 K and a fixed surface emissivity of 0.98. In addition, a perturbation method is also conducted, where 1 K for temperature and 5% for moisture are assumed. It is clear that three RTMs have similar Jacobian performances for the temperature profile but are quite different for the moisture profile. The TL scheme employed in cRTM and RTTOV produces results close to the perturbation method. The AA scheme based on monochromic assumption, however, results in much greater errors for the moisture Jacobian calculation. This result is in good agreement with Huang *et al*.'s (2002) conclusion that the relative absolute linearization error from the linear form with AA Jacobians is shown to be between two and four orders of magnitude larger than that from the linear form with exact analytic Jacobians. The Jacobian of surface skin temperature is presented in figure 2. The input atmospheric

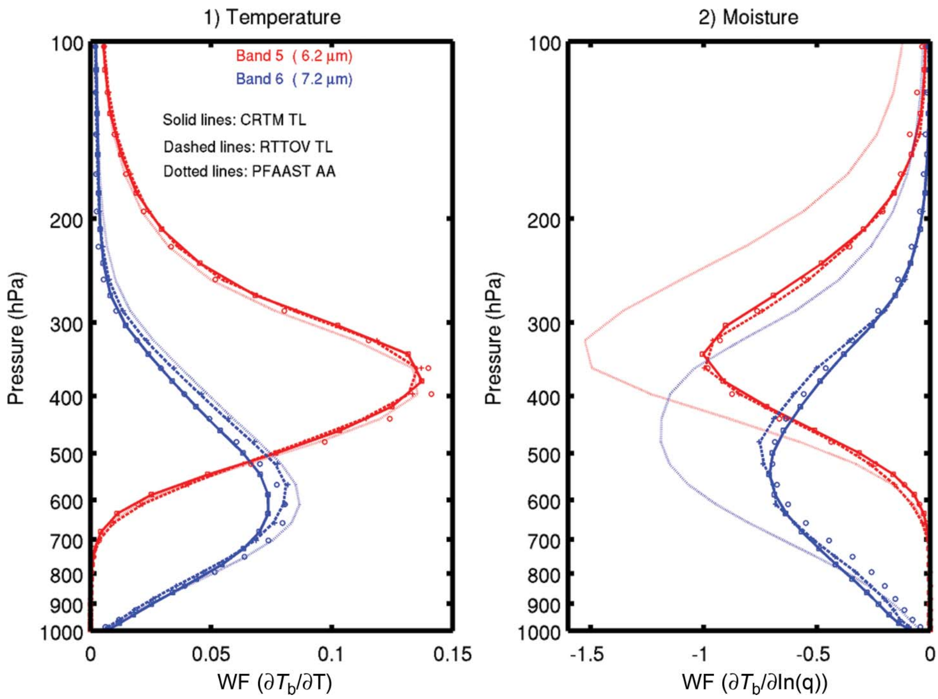

Figure 1. The temperature (left) and moisture (right) profile weighting function Jacobians for SEVIRI band 5 (6.2 µm, in red) and band 6 (7.3 µm, in blue) calculated from cRTM (solid), PFAAST (dotted) and RTTOV (dashed) respectively. Also plotted are Jacobians calculated using perturbation method by cRTM (square), PFAAST (circle) and RTTOV (cross).

and surface models are the same as those for figure 1. As in the the profile Jacobian calculation, the cRTM TL and RTTOV TL produce very similar results, and both of them are larger than those from the PFAAST AA method, indicating an advantage in retrieving surface skin temperature. The simulation of brightness temperatures (BTs) for seven SEVIRI IR channels is presented in figure 3. The input atmospheric and surface models are the same as those in figures 1 and 2, but the LZA changes between 0° and 65°. For most channels, the differences between the three RTMs are trivial. The largest difference occurs for the 7.3-µm channel: cRTM results in obviously larger BT than the other two models for all LZAs. The smaller the LZA is, the larger the difference. The real SEVIRI observations will be adopted to evaluate which RTM produces the best result in the next section.

The simulated profile and surface skin temperature retrievals are presented in figures 4 and 5 respectively. The LZA is fixed at 0 in the simulation. One-tenth of a profile data set, consisting of more than 15 700 global profiles of temperature, humidity and ozone (Seemann *et al*. 2008), is used in the simulation. The other 90% of this data set is used to generate the regression coefficient matrix. It is useful to explain that the GOES-R LAP retrieval algorithm is a two-step process: the first step is to generate a first guess of the profile and surface skin temperature using a predetermined non-linear regression coefficient matrix, taking satellite observations, forecast profiles and surface pressure, as well as some other variables such as month, latitude, LZA and land/water surface type, as predictors; the second step is to apply the one-dimension variation physical

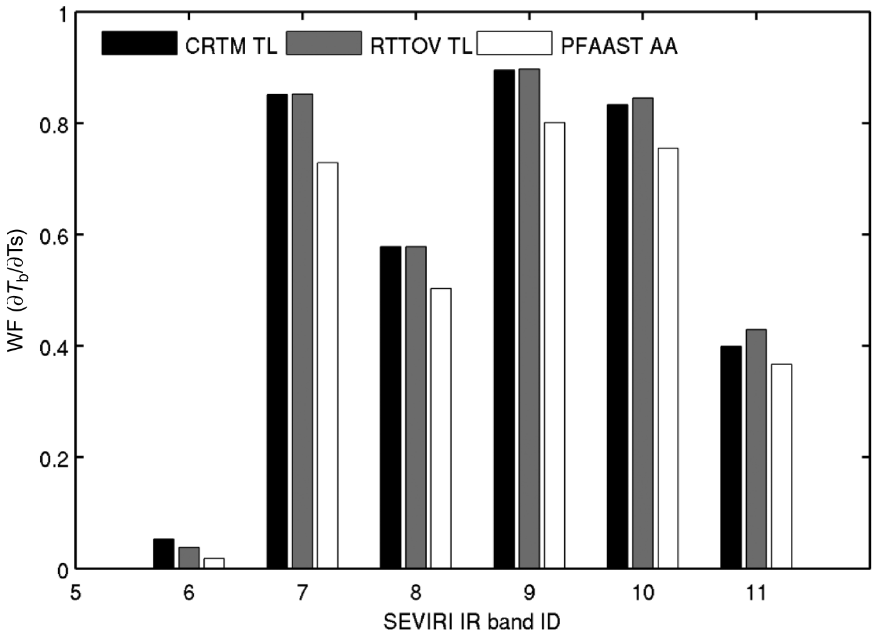

Figure 2. Jacobians of surface skin temperature for seven SEVIRI infrared bands derived from different RTMs.

retrieval (Jin *et al*. 2008). Three regression coefficient matrixes are generated using different RTMs. Since the simulated SEVIRI observations in the retrieval have no biases from those simulated in the training stage, the first guess has no effect using different RTMs. Therefore, it is not presented in figures 4 and 5. Another tricky point in the comparison concerns the vertical pressure ordinate. PFAAST is conducted in a fixed 101-level vertical pressure ordinate system, ranging between 0.005 hPa and 1100 hPa. RTTOV is operated in a 43-level vertical pressure ordinate system between 0.1 hPa and 1013.25 hPa. For cRTM, the pressure ordinate is adjustable within a maximal number of 101 levels. To make the results comparable, the retrieval with cRTM was conducted at two pressure ordinates: one the same as the PFAAST 101-level mode and the other the same as the RTTOV 43-level mode, marked as CRTM 101 and CRTM43 respectively in figure 4. As indicated in figure 1, the temperature profiles retrieved by the three models show almost no differences. However, the moisture profile from cRTM101 is slightly but constantly better than that from the PFAAST, illustrating the improvement from the Jacobian matrix. When turned into the 43-level mode, cRTM generates nearly the same result as that from RTTOV. The total precipitable WV (TPW) and its three components at different significant levels – WV1 (surface to 0.9), WV2 (0.9 to 0.7) and WV3 (0.7 to 0.3) – are routine products derived from the GOES-R LAP algorithm. The statistical description of the simulated retrieval results is listed in table 1.

The surface skin temperature (T_s) has a significant impact on the profile retrieval. It is updated in the physical iteration in the GOES-R LAP retrieval and therefore outputted as a by-product. Figure 5 illustrates the retrieval of T_s by simulation. Here a 3-K root-mean-square error (RMSE) is added to simulate the forecast T_s. The retrievals by CRTM in 101- and 43-pressure level modes are plotted in black and

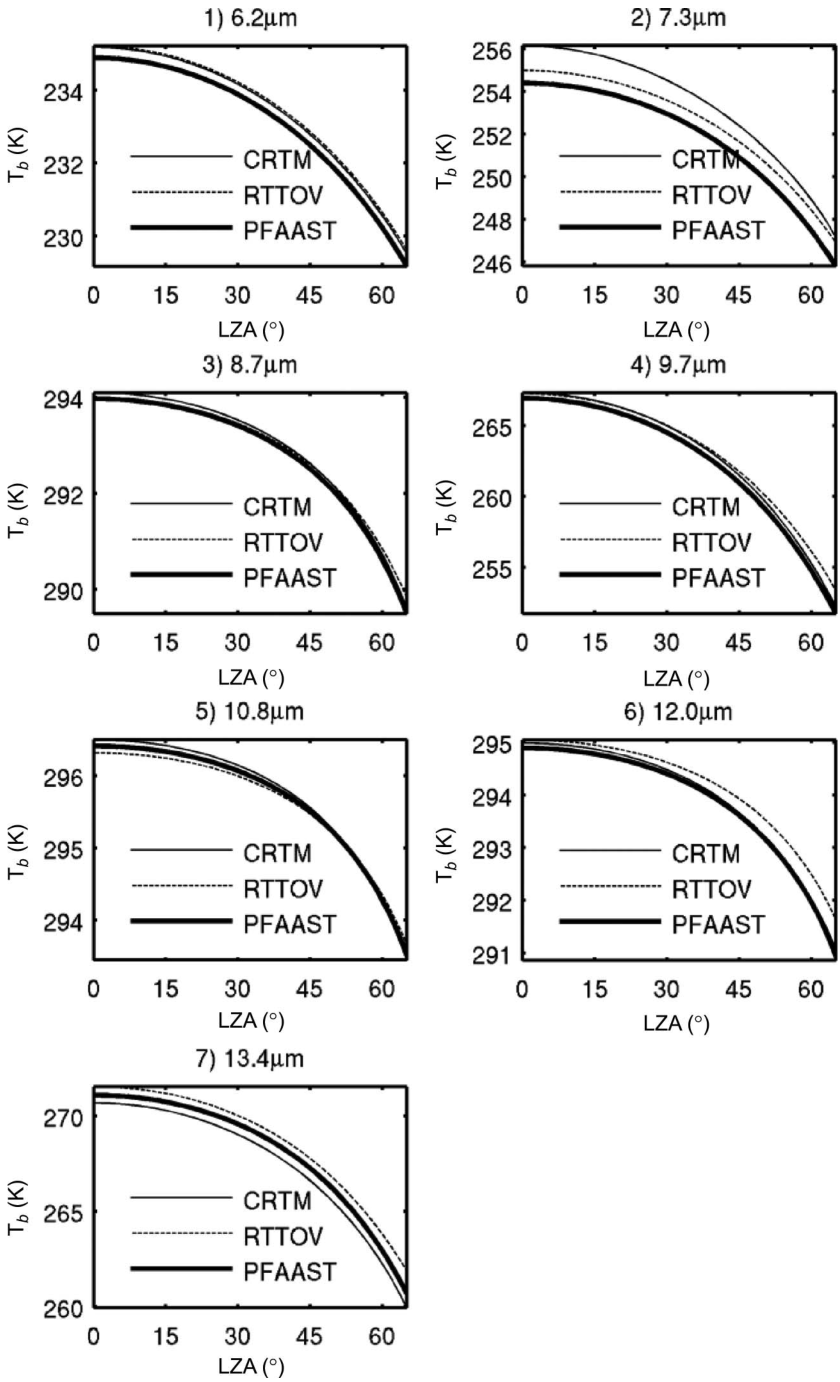

Figure 3. Simulated SEVIRI infrared brightness temperatures against the local zenith angle (LZA) with three RTMs.

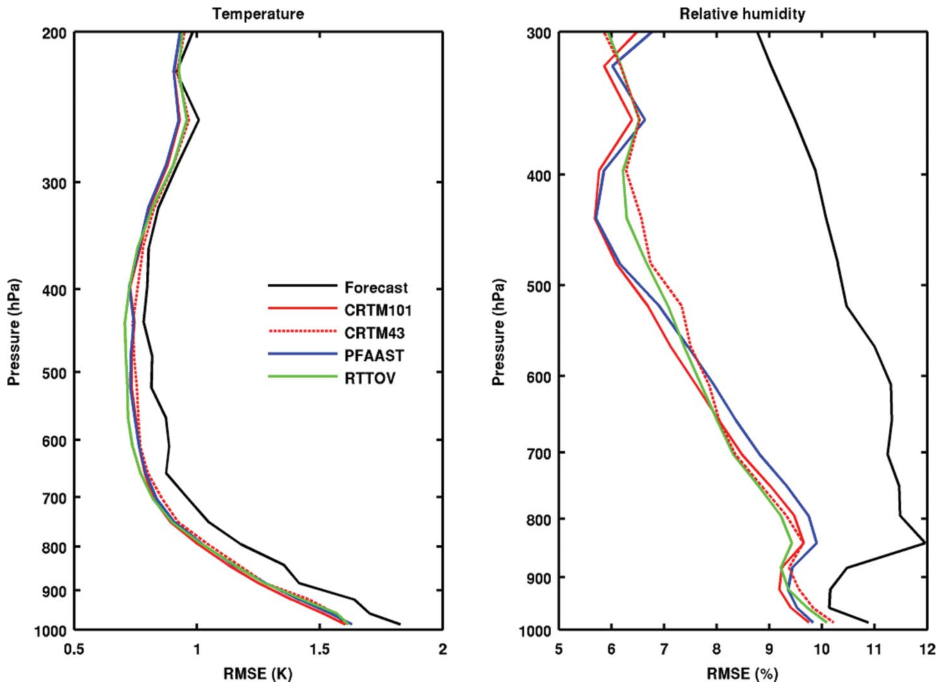

Figure 4. Simulation of temperature (left) and moisture (right) profile retrieval by cRTM (red), PFAAST (blue) and RTTOV (green) respectively in terms of root-mean-square error (RMSE) against the true. The forecast (black solid line) is also plotted. The cRTM retrieval is conducted in two pressure ordinates: a 101-level mode for comparison with PFAAST and a 43-level mode for comparison with RTTOV.

red respectively. The results clearly indicate the improvement after applying the TL method in cRTM and RTTOV.

2.2 *Case studies*

A total number of 457 SEVIRI clear-sky observations are collected with *in situ* radiosonde measurements at 00:00 and 12:00 Coordinated Universal Time (UTC) in August 2006 over land. Since the GOES-R LAP algorithm can only run in clear-sky pixels, a cloud-mask data set was ordered from the EUMETSAT (The European Organisation for the Exploitation of Meteorological Satellites) for clear-sky pixel identification. The SEVIRI data were downsized by averaging the clear-sky pixels in each 3×3 box. The locations of these samples are plotted in the bottom right of figure 6. The other three panels in figure 6 are the comparisons of BTs between the observations and calculations for three absorbing bands (6.3 μm, 7.3 μm and 13.4 μm) by cRTM, PFAAST and RTTOV using the *in situ* radiosonde profiles. It is clear that these RTMs have very similar performance for the 6.3-μm band, and cRTM is the best for the 7.3-μm band with the smallest RMSE and smallest negative bias. Considering that, according to figure 2, the cRTM-simulated BT is larger than the other two RTMs for all LZAs, it is clear that PFAAST and RTTOV have significant negative bias in simulating 7.3-μm BT. The reason of such a negative bias needs to be investigated further.

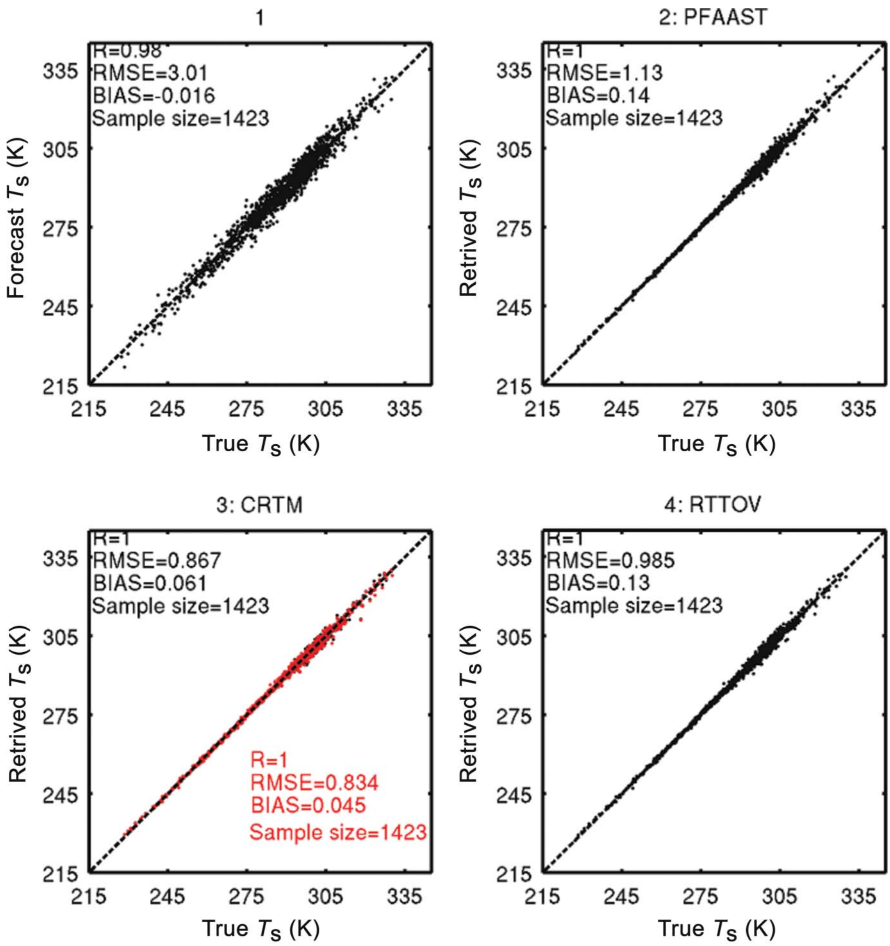

Figure 5. Simulation of surface skin temperature retrieval by different RTMs. Here, a 3-K standard variation is assumed in the simulation of the forecast skin temperature, and the cRTM retrieval is conducted in two pressure ordinates: a 101-level mode (black) for comparison with PFAAST and a 43-level mode (red) for comparison with RTTOV.

Table 1. The statistics of the simulated moisture retrieval by different RTMs.

	TPW			WV1			WV2			WV3		
	R	RMSE	BIAS	*R*	RMSE	BIAS	*R*	RMSE	BIAS	*R*	RMSE	BIAS
Forecast	0.98	3.63	0.42	0.97	1.41	−0.048	0.97	1.92	0.13	0.97	1.23	0.32
PFAAST	0.99	2.93	0.047	0.98	1.27	−0.096	0.98	1.62	0.051	0.99	0.729	0.089
CRTM101	0.99	2.76	0.053	0.98	1.24	−0.11	0.98	1.54	0.03	0.99	0.674	0.082
CRTM43	0.99	2.6	−0.17	0.98	1.29	−0.21	0.98	1.43	−0.041	0.99	0.685	0.086
RTTOV	0.99	2.67	−0.14	0.98	1.28	−0.22	0.98	1.47	0.0085	0.99	0.717	0.073

Note: *R* = correlation coefficient; RMSE = root-mean-square error (in mm); BIAS = mean bias (in mm); TPW = total water vapour content. WV1, WV2 and WV3 = integrated water vapour content at different significant levels: surface to 0.9, 0.9 to 0.7 and 0.7 to 0.3 respectively.

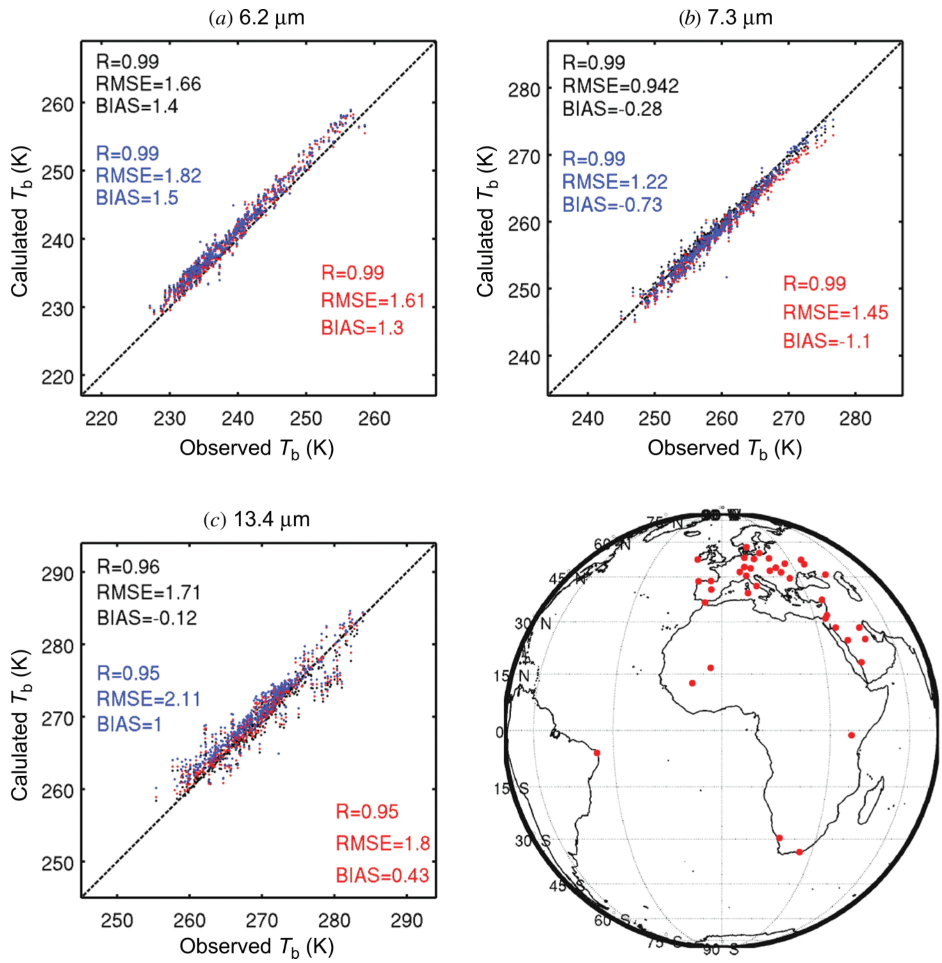

Figure 6. The comparison of brightness temperature for the SEVIRI band 5 (6.2 μm), 6 (7.3 μm) and 11 (13.4 μm) between the observations and the calculations over land. PFAAST is in red, RTTOV is in blue and cRTM is in black. The sampling sites are displayed in the bottom right.

For the 13.4-μm band, cRTM also has the best performance, although the result is impacted by the uncertainty of the surface temperature.

Since the result of moisture profile retrieval is inconsistent as the pressure ordinate changes, the retrieved profile RMSE against the rawinsonde data set is not presented. Instead, the statistics of retrieved TPW and WV1/WV2/WV3 against the true value from radiosonde is recorded in table 2. In this comparison, the forecast profiles are from the European Centre for Medium-Range Weather Forecasts (ECMWF) 12-h forecast product. Similar to table 1, the cRTM of the 101-level has better performance than PFAAST, especially for WV3, which is at the upper levels. The better simulation of 7.3-μm BT by cRTM101 leads to a significant reduction in BIAS. The cRTM43's results are very close to those of RTTOV.

Table 2. The statistics of the moisture retrieval by different RTMs using real data.

	TPW			WV1			WV2			WV3		
	R	RMSE	BIAS	*R*	RMSE	BIAS	*R*	RMSE	BIAS	*R*	RMSE	BIAS
Forecast	0.92	2.91	0.15	0.92	1.18	0.08	0.88	1.75	−0.021	0.88	1.23	0.086
PFAAST	0.94	2.69	−0.86	0.92	1.13	−0.027	0.89	1.68	−0.33	0.93	1.03	−0.52
CRTM101	0.94	2.57	−0.52	0.93	1.07	−0.094	0.9	1.62	−0.29	0.93	0.906	−0.16
CRTM43	0.94	2.58	−0.63	0.93	1.08	−0.17	0.9	1.65	−0.36	0.91	1.02	−0.12
RTTOV	0.93	2.71	−0.35	0.93	1.1	−0.082	0.89	1.65	−0.16	0.91	1.04	−0.12

3. Concluding remarks

Two fast RTMs, the cRTM and RTTOV, and their associated TL Jacobian schemes are tested in the GOES-R LAP retrieval algorithm and compared with the currently employed PFAAST and AA Jacobian scheme. It is found that that cRTM and RTTOV have similar and better Jacobian scheme than the currently used AA scheme. Another finding is that the cRTM has the best BT simulation for the 7.3-µm channel. Either RTTOV or cRTM is able to provide a better GOES-R LAP product than the currently used PFAAST. Integrating these RTMs and associated Jacobian schemes into ABI or SEVIRI profile retrieval algorithm will help improve the quality of retrieved atmospheric moisture information for climate study.

Acknowledgements
This study was partially supported by NOAA GOES-R Grant NA06NES4400002. The views, opinions and findings contained in this report are those of the authors, and should not be construed as an official National Oceanic and Atmospheric Administration or US government position, policy or decision.

References

Aires, F., Rossow, W.B., Scott, N.A. and Chedin, A., 2002, Remote sensing from the infrared atmospheric sounding interferometer instrument 2. Simultaneous retrieval of temperature, water vapor, and ozone atmospheric profiles. *Journal of Geophysical Research*, **107**, p. 4620.

Bates, J.J. and Jackson, D.L., 2001, Trends in upper tropospheric humidity. *Geophysical Research Letters*, **28**, pp. 1695–1698.

Bates, J.J., Wu, X. and Jackson, D.L., 1996, Interannual variability of upper-troposphere water vapor band brightness temperature. *Journal of Climate*, **9**, pp. 427–438.

Del Genio, A.D., Kovari Jr., W. and Yao, M.-S., 1994, Climatic implications of the seasonal variation of upper troposphere water vapor. *Geophysical Research Letters*, **21**, pp. 2701–2704.

Dessler, A.E., Yang, P., Lee, J., Solbrig, J., Zhang, Z. and Minschwaner, K., 2008, An analysis of the dependence of clear-sky top-of-atmosphere outgoing longwave radiation on atmospheric temperature and water vapor. *Journal of Geophysical Research*, **113**, p. D17102.

Divakarla, M.G., Barnet, C.D., Goldberg, M.D., McMillin, L.M., Maddy, E., Wolf, W., Zhou, L. and Liu, X., 2006, Validation of Atmospheric Infrared Sounder temperature and water vapor retrievals with matched radiosonde measurements and forecasts. *Journal of Geophysical Research*, **111**, p. D09S15.

GAFFEN, D.J., BARNETT, T.P. and ELLIOTT, W.P., 1991, Space and time scales of global tropospheric moisture. *Journal of Climate*, **4**, pp. 989–1008.

GUTZLER, D.S., 1992, Climatic variability of temperature and humidity over the tropical western Pacific. *Geophysical Research Letters*, **19**, pp. 1595–1598.

HAN, Y., VAN DELST, P., LIU, Q., WENG, F., YAN, B., TREADON, R. and DERBER, J., 2006, JCSDA Community Radiative Transfer Model (CRTM) – Version 1, *NOAA Technical Report*, **122**, p. 33.

HANNON, S., STROW, L.L. and MCMILLAN, W.W., 1996, Atmospheric infrared fast transmittance models: a comparison of two approaches. *Optical Spectroscopic Techniques and Instrumentation for Atmospheric and Space Research II. Proc. SPIE*, **2830**, pp. 94–105.

HARRIES, J.E., 1997, Atmospheric radiation and atmospheric humidity. *Quarterly Journal of the Royal Meteorological Society*, **123**, pp. 2173–2186.

HELD, I.M. and SODEN, B.J., 2000, Water vapor feedback and global warming. *Annual Review of Environment and Resources*, **25**, pp. 441–475.

HUANG, B., SMITH, W.L., HUANG, H.-L. and WOOLF, H.M., 2002, Comparison of linear forms of the radiative transfer equation with analytic Jacobians. *Applied Optics*, **41**, pp. 4209–4219.

JIN, X., LI, J., SCHMIT, T.J., LI, J., GOLDBERG, M.D. and GURKA, J.J., 2008, Retrieving clear sky atmospheric parameters from SEVIRI and ABI infrared radiances. *Journal of Geophysical Research*, **113**, p. D15310.

KIEHL, J.T. and TRENBERTH, K.E., 1997, Earth's annual global mean energy budget. *Bulletin of the American Meteorological Society*, **78**, pp. 197–208.

LI, J., 1994, Temperature and water vapor weighting functions from radiative transfer equation with surface emissivity and solar reflectivity. *Advance in Atmospheric Sciences*, **11**, pp. 421–426.

LI, J., WOLF, W., MENZEL, W.P., ZHANG, W., HUANG, H.-L. and ACHTOR, T.H., 2000, Global soundings of the atmosphere from ATOVS measurements: the algorithm and validation. *Journal of Applied Meteorology*, **39**, pp. 1248–1268.

LINDZEN, R., 1990, Some coolness concerning global warming. *Bulletin of American Meteorological Society*, **71**, pp. 288–299.

PEIXOTO, J. and OORT, A.H., 1996, Climatology of relative humidity in the atmosphere. *Journal of Climate*, **9**, pp. 3443–3463.

PICON, L., ROCA, R., SERRAR, S., MONGE, J.L. and DESBOIS, M., 2003, A new METEOSAT 'water vapor' archive for climate studies. *Journal of Geophysical Research*, **108**, p. 4301.

QIAN, W., ZHU, Y., XIE, A. and YE, Q., 1998, Seasonal and interannual variation of upper tropospheric water vapor band brightness temperature over the global monsoon regions. *Advances in Atmospheric Sciences*, **15**, pp. 337–345.

RANDEL, D.L., GREENWALD, T.J., VONDER HAAR, T.H., STEPHENS, G.L., RINGERUD, M.A. and COMBS, C.L., 1996, A new global water vapor dataset. *Bulletin of the American Meteorological Society*, **77**, pp. 1233–1246.

ROSSOW, W.B. and SCHIFFER, R.A., 1991, ISCCP cloud data products. *Bulletin of the American Meteorological Society*, **72**, pp. 2–20.

SAUNDERS, R., BRUNEL, P., CHEVALLIER, F., DEBLONDE, G., ENGLISH, S., MATRICARDI, M. and RAYER, P., 2002, RTTOV-7 science and validation report. *Met Office Technical Report FR-387*, 51 pp.

SCHMIT, T.J., GUNSHOR, M.M., MENZEL, W.P., GURKA, J., LI, J. and BACHMEIER, S., 2005, Introducing the next-generation advanced baseline imager (ABI) on GOES-R. *Bulletin of American Meteorological Society*, **86**, pp. 1079–1096.

SCHMIT, T.J., LI, J., ACKERMAN, S.A. and GURKA, J.J., 2009, High spectral and high temporal resolution infrared measurements from geostationary orbit. *Journal of Atmospheric and Oceanic Technology*, **26**, pp. 2273–2292.

SCHNEIDER, E.K., KIRTMAN, B.P. and LINDZEN, R.S., 1999, Tropospheric water vapor and climate sensitivity. *Journal of the Atmospheric Sciences*, **56**, pp. 1649–1658.

Seemann, S.W., Borbas, E.E., Knuteson, R.O., Stephenson, G.R. and Huang, H.-L., 2008, Development of a global infrared land surface emissivity database for application to clear sky sounding retrievals from multi-spectral satellite radiance measurements. *Journal of Applied Meteorology and Climatology*, **47**, pp. 108–123.

Sherlock, V., Collard, A., Hannon, S. and Saunders, R.W., 2003, The Gastropod Fast Radiative Transfer Model for advanced infrared sounders and characterization of its errors for radiance assimilation. *Journal of Applied Meteorology*, **42**, pp. 1731–1747.

Shine, K.P. and Sinha, A., 1991, Sensitivity of the earth's climate to height dependent changes in the water vapor mixing ratio. *Nature*, **354**, pp. 382–384.

Soden, B.J. and Schroeder, S.R., 2000, Decadal variations in tropical water vapor: a comparison of observations and a model simulation. *Journal of Climate*, **13**, pp. 3337–3341.

Wu, X., Bates, J.J. and Khalsa, S.J., 1993, A climatology of the water vapor brightness temperatures from NOAA operational satellites. *Journal of Climate*, **6**, pp. 1282–1300.

Zhai, P. and Eskridge, R.E., 1997, Atmospheric water vapor over China. *Journal of Climate*, **10**, pp. 2643–2652.